RSC Advances

ROYAL SOCIETY OF CHEMISTRY

www.rsc.org/advances

Graphic Abstract

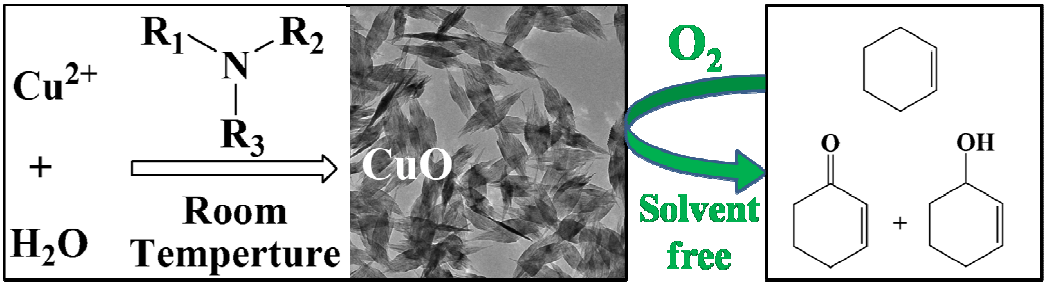

The CuO nanoleaves with a mesoporous structure have been synthesized in the presence of triethylamine at room temperature. The mesoporous CuO nanoleaves exhibit excellent catalytic activity for the solvent-free cyclohexene oxidation with oxygen.

Journal Name

ARTICLE

Room-temperature synthesis of mesoporous CuO and its catalytic activity for cyclohexene oxidation

Received 00th January 20xx,
Accepted 00th January 20xx

DOI: 10.1039/x0xx00000x

www.rsc.org/

Xinxin Sang, Jianling Zhang*, Tianbin Wu, Bingxing Zhang, Xue Ma, Li Peng, Buxing Han, Xinchen Kang, Chengcheng Liu, Guanying Yang

CuO nanoleaves with mesoporous structure were formed in aqueous solution of triethylamine at room temperature. The growth process of the CuO nanoleaves in triethylamine solution was investigated by varying reaction time. It is shown that the CuO nanostructures form by a reconstructive transformation from $Cu(OH)_2$, going through a 0 D nanoparticle $\rightarrow$1 D nanowire $\rightarrow$2 D nanoleaf dimensional transition process. The mechanism for the amine-induced formation of CuO at room temperature was studied by using different aliphatic amines. It is revealed that the amines play multiple roles on CuO formation, i.e. acting as alkali, dominating the $Cu(OH)_2$ to CuO transformation, and directing the oriented crystal growth of CuO. This route is simple, rapid, involves no additional alkalis or directing agents, and can proceed at room temperature. The as synthesized CuO exhibits excellent catalytic activity for cyclohexene oxidation with oxygen under solvent-free condition.

1. Introduction

Cupric oxide (CuO) is one of the transition metal oxides with interesting properties, such as nontoxicity, low-cost, and easy availability.[1] CuO with controlled morphology and size has attracted much attention because of its diverse applications in catalysis,[2-7] batteries,[8-11] solar cells,[12,13] supercapacitors,[14,15] sensors,[16-18] photodetectors,[19,20] etc. On one hand, CuO in nano-scale can provide unique size-dependent physical and chemical properties, large surface area and quantum size effects.[21] Numerous efforts have been devoted to the fabrication of nanostructured CuO with controllable size and morphology.[1] On the other hand, the introduction of mesoporosity in CuO can drastically enhance the surface properties of CuO material and manifest good conductivity and permeability for many important technological applications.[3,9-11,22-24] For example, the mesoporous CuO exhibits high activity for catalyzing chemical reactions (e.g. CO oxidation, epoxidation of alkenes, decomposition of H_2O_2)[3,22-24] and improves the electrochemical performance for lithium-ion batteries.[9-11] The combination of nanostructure and mesoporous structure will confer CuO special properties, which is very promising in view of its applications in different fields. However, the reports on the fabrication of mesoporous CuO nanostructure are very limited and the reported methods suffer from either utilizing templating agent[25-28] or high temperatures.[29-35] To explore the facile synthesis of mesoporous CuO nanocrystals at room temperature is of great importance, but still remains challenging.

Amines are organic compounds containing a basic N atom with a lone pair of electrons which are closely related to ammonia. The organic amines have been widely used in the controlled synthesis of metal, metal oxide, quantum dots, etc.[36] The basicity and affinity to metals through their NH_2 functional groups make amines versatile in modulating the morphology and crystallinity of nanoparticles.[37,38] The most adopted amines for nanoparticle synthesis are long-chain alkylamines, such as oleylamine,[39] hexadecylamine[40,41] octadecylamine,[42] bis-(amidoethyl-carbamoylethyl) octadecylamine.[43] It has been recognized that the long-chain alkylamines act as a surfactant (or a face selective adsorption additive) to control the orientated growth of nanoparticles. In contrast, the reports on using short-chain alkylamines for nanoparticle fabrication are much less.[44,45]

Here we explored the performance of short-chain aliphatic amines on the CuO nanostructure formation at room temperature. CuO nanoleaves with mesoporous structure were formed in aqueous solution of triethylamine (TEA). The reaction process was found to go through a reconstruction transformation from $Cu(OH)_2$ nanowires to CuO nanoleaves. A series of alkylamines were tested for CuO synthesis. It is revealed that the amines play multiple roles on CuO formation: 1) act as alkali, 2) dominate the $Cu(OH)_2$ to CuO

X. Sang, Prof. J. Zhang, T. Wu, B. Zhang, X. Ma, L. Peng, Prof. B. Han, X. Kang, C. Liu, G. Yang
Beijing National Laboratory for Molecular Science
CAS Key Laboratory of Colloid and Interface and Chemical Thermodynamics
Institute of Chemistry
Chinese Academy of Sciences (China)
E-mail: zhangjl@iccas.ac.cn
Electronic Supplementary Information (ESI) available: [details of any supplementary information available should be included here]. See DOI: 10.1039/x0xx00000x

transformation, 3) direct the oriented crystal growth of CuO. This route is simple, rapid, involves no additional alkali or directing agent, and can proceed at room temperature. The as synthesized CuO combines the advantages of the nanostructure and mesoporous structure, and has shown high activity in catalyzing the oxidation of cyclohexene with oxygen under solvent-free conditions.

2. Experimental

2.1 Materials

O_2 (>99.95%) was provided by Beijing Analysis Instrument Factory. Copper (II) salts such as Copper (II) acetate monohydrate ($Cu(OAc)_2 \cdot H_2O$), copper sulfate ($CuSO_4$), copper nitrate ($Cu(NO_3)_2$) and copper chloride ($CuCl_2$), (A. R. Grade) were purchased from Alfa Aesar. Triethylamine (TEA), diethylamine (DEA), 70 wt% aqueous solution of ethylamine (EA), 25 wt% aqueous solution of trimethylamine (TMA), tripropylamine (TPA), tributylamine (TBA), commercial CuO, cyclohexene and n-heptane were purchased from J&K scientific Co. Ltd. All these materials were used without further purification.

2.2 Synthesis

For a typical synthesis, $Cu(Ac)_2$ H_2O (2 mmol) was dissolved in 10 g H_2O, then amine (7.2 mmol) was added into the aqueous solution. The mixture was stirred at room temperature for the desired time. After centrifugation, washing with distilled water and ethanol several times and drying at 60 °C for 24 h under vacuum, the product was collected.

2.3 Characterization

The morphologies of the products were characterized by SEM (HITACHI S-4800), TEM (JEOL JEM-1011) and Field Emission Transmission Electron Microscopy (JEOL JEM-2100F). XRD pattern was performed on a Rigaku D/max-2500 diffractometer with Cu Kα radiation (λ= 1.5418 Å) at 40 kV and 200 mA. The porosity properties were gained from nitrogen adsorption-desorption isotherms using a Micromeritics ASAP 2020(M + C) system. FT-IR spectra were obtained by a Bruker Tensor 27 spectrometer. X-ray photoelectron spectroscopy (XPS) data were obtained with an ESCALab220i-XL electron spectrometer from VG Scientific using 300W AlKα radiation. The base pressure was about 3×10^{-9} mbar. The binding energies were referenced to the C1s line at 284.8 eV from adventitious carbon.

2.4 Catalytic test

In a typical oxidation reaction, 2 mL cyclohexene and 20 mg catalyst were placed into a round bottomed flask with condenser. The reaction system was then heated to 80 ^{o}C in oil bath under oxygen pressure and maintained at this temperature for different time under stirring. After reaction, the reactor was cooled to room temperature and the liquid phase was separated from the reaction slurry. The liquid samples were analyzed by gas chromatography (GC) with an SE-54 capillary column (30 m×0.32 mm×0.5 μm) and a flame ionization detector (FID). N-heptane was used as the internal standard for product analysis. For the reusability investigation, after reaction for 10 h, the catalyst was recovered by centrifugation, washed with ethanol several times and dried under vacuum. Then the solid was reused for a consecutive run.

3. Results and discussion

3.1 CuO prepared in TEA solution

The CuO typically prepared in TEA solution at room temperature for 24 h was characterized by XRD, SEM and TEM, and the results are shown in Fig. 1. The XRD pattern (Fig. 1a) shows that all the diffraction peaks are indexed to the standard monoclinic symmetry of CuO (JCPDS file no. 48-1548). The broad diffraction peaks indicate the nanocrystalline nature of the synthesized CuO. No peaks of impurities such as copper hydroxide or other copper compounds are detected, suggesting the high purity of the as-prepared product. The typical SEM and TEM images of the CuO are shown in Fig. 1b-g. The CuO crystal has a leaf-like architecture with dimensions of 100 nm in width, 400 nm in length and 10 nm in thickness. The magnified TEM image shown in Fig. 1e reveals that the CuO nanoleaf has a mesoporous structure. From Fig. 1f, the spherical mesopores with the size of 2.7±0.9 nm can be clearly observed. The high-resolution TEM (HRTEM) image shown in Fig. 1g demonstrates a clear and continuous lattice-fringe, indicating that the CuO nanoleaf has the same crystallographic orientation and is single-crystalline. The lattice spacing (0.232 nm) corresponds to the (111) facet of standard monoclinic symmetry of CuO crystal, which is in good agreement with XRD result shown in Fig. 1a. The CuO was further characterized by FT-IR and XPS spectra (Fig. S1, S2), which prove the absence of TEA in the product.

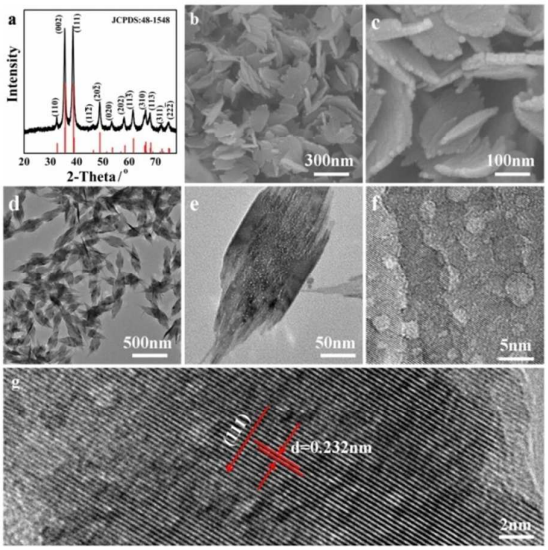

Fig. 1 XRD (a), SEM (b, c) and TEM (d-g) images of CuO prepared in TEA solution for 24 h.

The porosity property of the CuO was investigated by N_2 adsorption-desorption method. As shown in Fig. 2, the N_2 adsorption-desorption isotherm exhibits a mode of type IV, which indicates that the as-synthesized CuO is mesoporous. The BET (Brunauer, Emmett, and Teller) surface area and total pore volume of the CuO synthesized in TEA solution are 90.62 $m^2\ g^{-1}$ and 0.490 $cm^3 \cdot g^{-1}$, respectively. The mesopore size distribution curve, calculated from Barrett-Joyner-Halenda method, shows a pore size distribution centered at around 2.3 nm (inset of Fig. 2), which is consistent with the result from TEM observation.

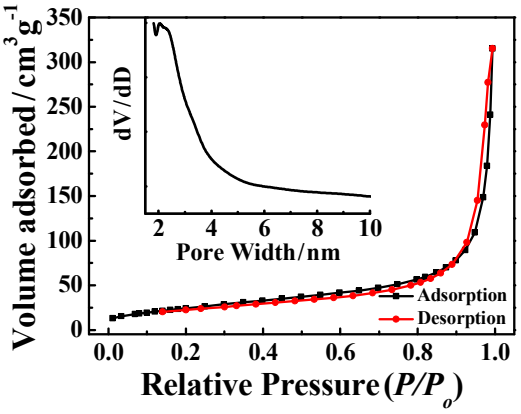

Fig. 2 N_2 adsorption-desorption isotherm and mesopore size distribution curve (the inset) of mesoporous CuO nanoleaves prepared in TEA solution at room temperature for 24 h.

3.2 Effect of reaction time

The growth process of the CuO nanoleaves in TEA solution was investigated by varying reaction time. At the initial stage of reaction (5 min), nanowires in diameter of 2-3 nm and length ranging from tens to hundreds nanometers were formed (Fig. 3a). It is noteworthy that many colloidal particles on nanoscale (~3 nm) line together to form the wire-like materials (Fig. 3e). The nanowires obtained at this stage are amorphous, as evidenced by XRD pattern (black line in Fig. 3i). As the reaction progresses (1 h), some thin nanoleaves with width of 30 nm and length of 140 nm appear among the nanowires (Fig. 3b, f), corresponding to a mixture of orthorhombic $Cu(OH)_2$ and monoclinic CuO (red line in Fig. 3i). Longer reaction time (9 h) results in the growth of the nanoleaves to 80 nm in width and 300 nm in length (Fig. 3c, g). The orthorhombic $Cu(OH)_2$ and monoclinic CuO still coexist at this stage (green line in Fig. 3i). After reaction for 18 h, the nanowires disappear completely and the product is composed of nanoleaves with width in 80 nm and length in 350 nm (Fig. 3d, h). The XRD result proves that the product is composed of pure CuO phase (blue line in Fig. 3i). In comparison with Fig. 1, it can be seen that the CuO synthesized at 18 h is a little smaller than that synthesized at 24 h. The above results indicate that the CuO may form by a reconstructive transformation from $Cu(OH)_2$, going through a 0 D nanoparticle → 1 D nanowire →2 D nanoleaf dimensional transition process.

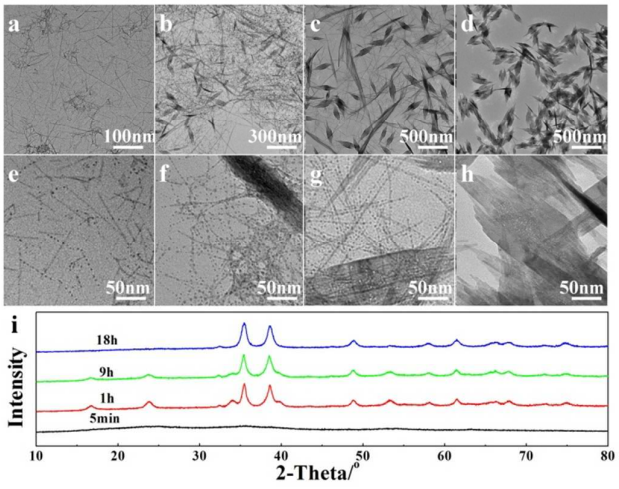

Fig. 3 TEM images of the products obtained at 5 min (a, e), 1 h (b, f), 9 h (c, g), and 18 h (d, h). (i) XRD patterns of the products obtained at 5 min (black), 1 h (red), 9 h (green) and 18 h (blue).

3.3 Effect of different amines

Further, tertiary amines with different length of alkyl groups, TMA, TPA, TBA were used as alternatives of TEA to prepare CuO nanostructures. The reaction time was fixed at 24 h. Pure CuO with the morphology similar to that formed in TEA was obtained in TMA (Fig. S3, S4). However, TPA and TBA produce a blend of CuO nanoleaves and $Cu(OH)_2$ nanobundles (Fig. S3, S4). The results prove that the amine plays a decisive role in producing CuO, i.e. the tertiary amine with the shorter alkyl chain length is favorable for the transformation from $Cu(OH)_2$ to CuO, and vice versa. Further, DEA and EA with different number H of ammonia substituted by ethyl groups were used to synthesize CuO, the experimental conditions being the same with those above. The blend of CuO nanoleaves and $Cu(OH)_2$ nanobundles was formed in DEA, while pure $Cu(OH)_2$ nanobundles were obtained in EA (Fig. S3, S5). All these data are summarized in Table 1.

Table 1. Products synthesized in different amine solutions.

Amine	Molecular structure	pH	Product	Morphology
Trimethylamine (TMA)		11.25	CuO	Nanoleaves
Triethylamine (TEA)	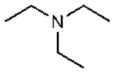	11.08	CuO	Nanoleaves
Tripropylamine (TPA)	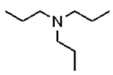	10.28	$Cu(OH)_2$ +CuO	Nanobundles +Nanoleaves
Tributylamine (TBA)	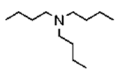	9.28	$Cu(OH)_2$ +CuO	Nanobundles +Nanoleaves
Diethylamide (DEA)	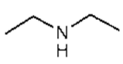	11.65	$Cu(OH)_2$ +CuO	Nanobundles +Nanoleaves

Ethylamine (EA)	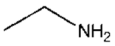	11.72	$Cu(OH)_2$	Nanobundles

In the wet-chemical route for synthesizing CuO, the varied pH value can tailor the morphologies and dimensions of CuO nanostructures.[46-50] Here we determined the pH values of the amine solutions and the results are listed in Table 1. The pH values of the aqueous solution of the six amines are in the order of EA>DEA>TMA>TEA>TPA>TBA. It is evident that a moderate pH range (11.08 and 11.25 for TEA and TMA, respectively) is favorable for CuO formation, while $Cu(OH)_2$ is formed at lower or higher pH value. This result is consistent with that reported in literature, which used sodium oleate as the surfactant and shape controller for the synthesis of CuO nanocrystals in aqueous solution.[50] By using NaOH to tune the alkalinity, a highest reaction velocity exists around pH 10.8, while the pH 10.6 and 11.0 slow down the speed for producing CuO.[50]

3.4 Effect of different copper salts

The CuO formation in TEA using $CuSO_4$, $Cu(NO_3)_2$ and $CuCl_2$ as copper salts was investigated. The results show that CuO can be formed from all these salt aqueous solutions at room temperature with the assistance of TEA (Fig. S6). The CuO samples synthesized from these three copper precursors appear as mesoporous nanoleaves (Fig. 4), similar to that obtained from $Cu(OAc)_2$. However, the CuO samples produced from the four cooper precursors are different in the aspect ratios of the nanoleaves. The CuO nanoleaves synthesized from $CuCl_2$ have the largest aspect ratio. It indicates that the anions of copper salt influence mainly on the size of CuO nanoleaves.

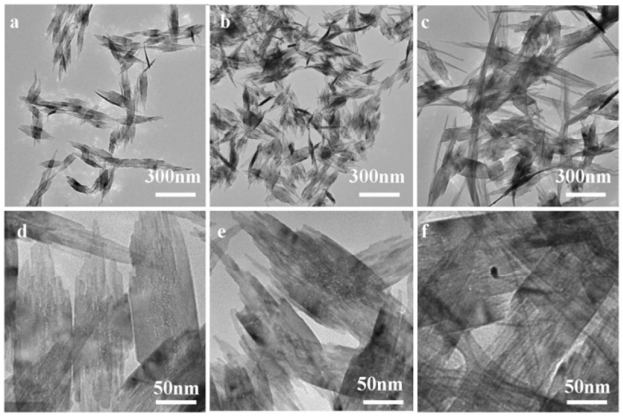

Fig. 4 TEM images of the CuO synthesized from $Cu(NO_3)_2$ (a, d), $CuSO_4$ (b, e) and $CuCl_2$ (c, f) in TEA aqueous solution.

3.5 Formation mechanism

Based on the above results, the amine-induced formation of CuO at room temperature is described as follows (Scheme 1). At the early stage, 1 D $Cu(OH)_2$ nanowires are formed, as revealed by TEM images shown in Fig. 3. The formation of $Cu(OH)_2$ nanowires with an orthorhombic phase in strong basic conditions is a common phenomenon, due to the coordination self-assembly of $Cu(OH)_4^{2-}$ ions during decomposition.[50] The amine dominates the transformation of $Cu(OH)_2$ to CuO. For TEA and TMA, the amines can form hydrogen bonding interactions with $Cu(OH)_4^{2-}$, which is beneficial to the dehydration of $Cu(OH)_2$ to form CuO (Route 1 in Scheme 1). CuO is likely to crystallize around $Cu(OH)_2$ nanoparticles, which act as templates for mesopore formation. The mesopores are thus formed after all $Cu(OH)_2$ dissolves for reconstruction. At the same time, CuO goes through an oriented crystal growth directed by amines. Therefore, CuO nanoleaves with mesoporous structures were obtained with the aid of TEA and TMA. As for TPA and TBA, the steric hindrance effect caused by the longer alky chains of these two amines could weaken the hydrogen bonding interactions with $Cu(OH)_4^{2-}$, unfavorable for the dehydration of $Cu(OH)_2$. Consequently, $Cu(OH)_2$ partly transforms to CuO and a blend of CuO and $Cu(OH)_2$ were obtained. Nevertheless, in the presence of EA or DEA, $Cu(OH)_4^{2-}$ is more likely to associate with the hydrogen atoms in $-NH_2$ or -NH due to the oxidation tendency of amines.[45] The attached amines in this way would hinder the dehydration, which is more favorable for the stabilization of $Cu(OH)_2$ (Route 2 in Scheme 1).

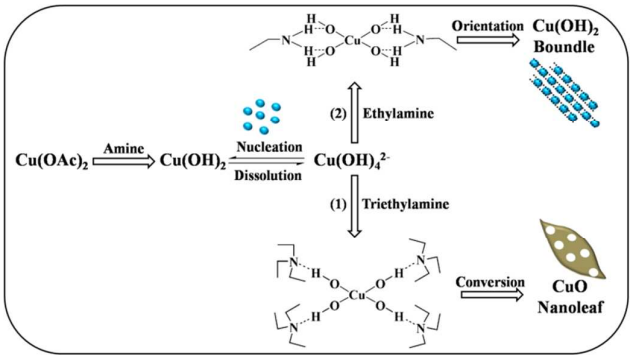

Scheme 1. Postulated mechanism for amine-induced CuO or $Cu(OH)_2$ formation.

3.6 Catalytic analysis

The oxidation of cyclohexene is an essential chemical process due to the potential uses of the products, including 2-cyclohexene-1-ol, and 2-cyclohexene-1-one.[51] The solvent-free oxidation of cycloolefins with clean oxidant oxygen is highly desirable from an ecological point of view, which also offers considerable synthetic advantages in terms of simplicity for the reaction procedure.[52] Different heterogeneous catalysts such as supported noble metal nanoparticles (e.g. Au, Pt and Ag),[53,54] Schiff-base transition metal complexes,[55,56] and metal-organic frameworks (MOF)[57-59] have been used for the solvent-free oxidation of cyclohexene with oxygen. The maximum conversions of cyclohexene over these catalysts are less than 50%. Also, in view of the high cost of noble metals, complex preparation of Schiff-base transition metal complex, and low catalytic activity of MOFs, it is urgent to develop highly efficient, easily prepared and low-cost catalyst for the oxidation of cyclohexene with oxygen in solvent-free conditions.

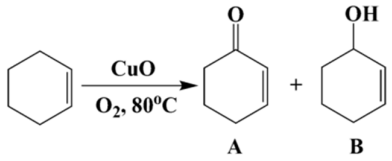

Scheme 2. Aerobic oxidation of cyclohexene catalyzed by CuO.

It has been reported that the catalytic activities of copper and its oxides show a dependence on both the microstructure and nanostructure of the catalyst.[60,61] CuO nanostructures typically have higher catalytic activity than their bulk or micro counterparts caused by their large surface area. The mesoporous CuO nanoleaves synthesized in this work combine the advantages of nanostructure and mesoporous structure, making it promising candidate for catalysis. Here the mesoporous CuO nanoleaves were used as catalyst for solvent-free oxidation of cyclohexene with oxygen as the only oxidant. It is a complex radical-chain reaction and cyclohexenyl peroxyl radical is the main chain propagator.[57] The molar ratio of catalyst to reactant was 0.013, the temperature was 80 °C, and the pressure of oxygen was 1 atm. The main products over CuO are 2-cyclohexen-1-one and 2-cyclohexen-1-ol (Scheme 2), derived from the decomposition of intermediate product 2-cyclohexene-1-hydroperoxide.[57] Other possible products like cyclohexene hydroperoxide, 2,3-epoxy-cyclohexanone, phenol or cyclohexene dimer were not detected. As shown in Table 2, the conversion of cyclohexene over CuO increases with the reaction time and reaches a conversion of 66.8% at reaction time 10 h (Entries 1-4). Then the conversion keeps nearly unchanged as the reaction time is prolonged to 15 h (Entries 5, 6). The oxidation of cyclohexene to give 2-cyclohexen-1-one predominates over CuO. In the first 12 h, the selectivity of 2-cyclohexen-1-one increases with the reaction time, while that of 2-cyclohexen-1-ol keeps almost unchanged (Entries 1-5). At 12 h, the total selectivities to 2-cyclohexen-1-one and 2-cyclohexen-1-ol can reach 90.3% (Entry 5). After that, the selectivities to 2-cyclohexen-1-one and 2-cyclohexen-1-ol decrease (Entry 6), indicative of the occurrence of a secondary reaction involving the transformation of 2-cyclohexen-1-one and 2-cyclohexen-1-ol to give other products.[56] When the molar ratio of catalyst to reactant is increased to 0.065, the cyclohexene conversion and the selectivities to 2-cyclohexen-1-one and 2-cyclohexen-1-ol keep nearly unchanged (Entry 7).

Table 2. Solvent-free oxidation of cyclohexene at 1 atm O_2.

Entry	Catalyst	Time /hour	Conversion /%	Selectivity/% A	B
1[a]	CuO	4	17.7	47.4	35.7
2[a]	CuO	6	52.8	51.4	33.7
3[a]	CuO	8	57.6	53.5	32.2
4[a]	CuO	10	66.8	54.8	33.3
5[a]	CuO	12	67.5	54.9	35.4
6[a]	CuO	15	66.8	46.8	28.7
7[b]	CuO	10	65.5	56.8	31.5
8[c]	CuO	10	71.8.	49.6	39.0
9[d]	CuO	10	70.5	52.1	34.6
10[e]	CuO	10	75.4	49.3	42.9
11	Commercial CuO	10	16.8	45.0	41.2

[a] CuO synthesized from $Cu(OAc)_2$. Reaction conditions: 0.020 g catalyst, 2 mL cyclohexene, the molar ratio of catalyst to reactant 0.013, 80 °C, 1 atm oxygen.
[b] The molar ratio of catalyst to reactant was 0.065, the other reaction conditions being the same with those of "a".
[c, d, e] CuO synthesized from $Cu(NO_3)_2$, $CuSO_4$, $CuCl_2$, respectively.

The catalytic performances of the CuO synthesized from different copper precursors were also tested, the experimental conditions being the same with those of Entry 4. As shown in Table 2 (Entries 8-10), the CuO nanoleaves with the largest aspect ratio synthesized from $CuCl_2$ have higher catalytic activity than others. The total selectivities to 2-cyclohexen-1-one and 2-cyclohexen-1-ol can reach 92.1% (Entry 10). For comparison, the catalytic performance of commercial CuO for the oxidation of cyclohexene was tested, the experimental conditions being the same with those of Entry 4. The conversion of cyclohexene catalyzed by commercial CuO is 16.8% at 10 h (Entry 11), significantly lower than that catalyzed by the mesoporous CuO nanoleaves synthesized in this work (66.8%, Entry 4). There is no obvious difference in the total selectivities to 2-cyclohexen-1-one and 2-cyclohexen-1-ol catalyzed by the two catalysts. The commercial CuO was characterized by TEM image and N_2 adsorption-desorption method, showing agglomerate in micron (Fig. S7) with a BET surface area as low as 2.04 $m^2 g^{-1}$ (Fig. S8). The high catalytic activities of the CuO synthesized in this work can be explained from the following two aspects. First, the nanoscale size of the CuO is favorable to increasing the density of catalytic active sites.[62] Second, the mesoporous structure of the CuO can enhance the diffusion of substrates and products.[63]

The reusability of CuO nanoleaves for solvent-free oxidation of cyclohexene was investigated. As shown in Fig. 5, the catalyst shows no evident drop of catalytic activity after four runs, indicating the high stability of CuO nanoleaves. The TEM image of CuO after reused four runs shows that the mesopores and nanostructures are both well preserved (Fig. S9).

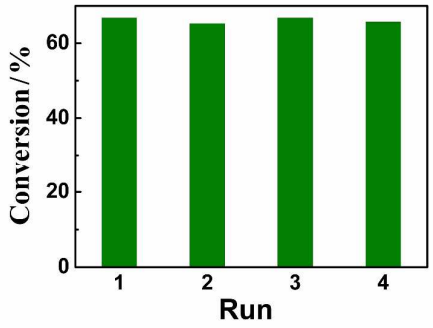

Fig. 5 Reusability of the CuO. Reaction conditions: 0.020 g CuO, 2 mL cyclohexene, 80 °C, 1 atm oxygen, reaction time 10 h.

Conclusions

Here the performance of a series of short-chain aliphatic amines on the CuO nanostructure formation was investigated for the first time. The presence of TMA and TEA favors the formation of single-crystalline CuO nanoleaves with a

mesoporous structure at room temperature. The amine plays a multiple role on CuO formation. First, amine acts as alkali to allow the reaction to proceed. Second, amine promotes the transformation of $Cu(OH)_2$ to CuO at room temperature. It is worth noting that the transformation from $Cu(OH)_2$ to CuO in aqueous solution at room temperature cannot frequently happen without special additives. Third, amine directs the oriented crystal growth of CuO and results in the final formation of CuO nanoleaves. This route excels the conventional methods for CuO nanocrystal formation, because it involves no additional alkali or directing agent and can proceed at room temperature. The as-synthesized CuO combines the advantages of nanostructure and mesoporous structure, and is expected to find more applications in catalysis, lithium-storage, etc.

Acknowledgements

This work was supported by National Natural Science Foundation of China (21173238, 21133009, U1232203, 21321063, 21373230) and Chinese Academy of Sciences (KJCX2.YW.H16).

Notes and references

1 Q. Zhang, K. Zhang, D. Xu, G. Yang, H. Huang, F. Nie, C. Liu and S. Yang, *Prog. Mater. Sci.*, 2014, **60**, 208.
2 L. Rout, T. K. Sen and T. Punniyamurthy, *Angew. Chem. Int. Ed.*, 2007, **46**, 5583.
3 L. Xu, S. Sithambaram, Y. Zhang, C. H. Chen, L. Jin, R. Joesten and S. L. Suib, *Chem. Mater.*, 2009, **21**, 1253.
4 H. Cao, H. F. Jiang, X. S. Zhou, C. R. Qi, Y. G. Lin, J. Y. Wu and Q. M. Liang, *Green Chem.*, 2012, **14**, 2710.
5 S. K. Rout, S. Guin, J. Nath and B. K. Patel, *Green Chem.*, 2012, **14**, 2491.
6 Q. Zhang, H. Y. Wang, X. Jia, B. Liu and Y. Yang, *Nanoscale*, 2013, **5**, 7175.
7 S. Ghosh, M. Roy and M. K. Naskar, *Cryst. Growth Des.*, 2014, **14**, 2977.
8 M. K. Song, S. Park, F. M. Alamgir, J. Cho and M. Liu, *Mater. Sci. Eng. R-Rep.*, 2011, **72**, 203.
9 B. Wang, X. L. Wu, C. Y. Shu, Y. G. Guo and C. R. Wang, *J. Mater. Chem.*, 2010, **20**, 10661.
10 S. Ko, J. I. Lee, H. S. Yang, S. Park and U. Jeong, *Adv. Mater.*, 2012, **24**, 4451.
11 H. Huang, Y. Liu, J. Wang, M. Gao, X. Peng and Z. Ye, *Nanoscale*, 2013, **5**, 1785.
12 A. Kargar, Y. Jing, S. J. Kim, C. T. Riley, X. Pan and D. Wang, *ACS Nano*, 2013, **7**, 11112.
13 Y. Xia, X. Pu, J. Liu, J. Liang, P. Liu, X. Li and X. Yu, *J. Mater. Chem. A*, 2014, **2**, 6796.
14 G. Wang, L. Zhang and J. Zhang, *Chem. Soc. Rev.*, 2012, **41**, 797.
15 S. Faraji and F. N. Ani, *J. Power Sources*, 2014, **263**, 338.
16 R. K. Bedi and I. Singh, *ACS Appl. Mater. Interfaces*, 2010, **2**, 1361.
17 A. Taubert, F. Stange, Z. Li, M. Junginger, C. Gunter, M. Neumann and A. Friedrich, *ACS Appl. Mater. Interfaces*, 2012, **4**, 791.
18 H. J. Kim and J. H. Lee, *Sens. Actuator B-Chem.*, 2014, **192**, 607.
19 W. Tian, C. Zhi, T. Zhai, X. Wang, M. Liao, S. Li, S. Chen, D. Golberg and Y. Bando, *Nanoscale*, 2012, **4**, 6318.
20 X. Zhang, W. Shi, J. Zhu, D. J. Kharistal, W. Zhao, B. S. Lalia, H. H. Hng and Q. Yan, *ACS Nano*, 2011, **5**, 2013.
21 Y. Yin, R. M. Rioux, C. K. Erdonmez, S. Hughes, G. A. Somorjai and A. P. Alivisatos, *Science*, 2004, **304**, 711.
22 X. Chen, N. Zhang and K. Sun, *J. Mater. Chem.*, 2012, **22**, 13637.
23 S. Ghosh and M. K. Naskar, *RSC Adv.*, 2013, **3**, 13728.
24 C. R. Jung, J. Han, S. W. Nam, T. H. Lim, S. A. Hong and H. I. Lee, *Catal. Today*, 2004, **93**, 183.
25 S. Ghosh, M. Roy and M. K. Naskar, *Cryst. Growth Des.*, 2014, **14**, 2977.
26 Y. X. Zhang, M. Huang, M. Kuang, C. P. Liu, J. L. Tan, M. Dong, Y. Yuan, X. Zhao and Z. Wen, *Int. J. Electrochem. Sci.*, 2013, **8**, 1366.
27 J. Guo, L. Ma, X. Zhang, Y. Zhang and L. Tang, *Mater. Lett.*, 2014, **118**, 142.
28 X. Lai, X. Li, W. Geng, J. Tu, J. Li and S. Qiu, *Angew. Chem. Int. Ed.*, 2007, **46**, 738.
29 M. F. Wang, Q. A. Huang, X. Z. Li and Y. Wei, *Anal. Methods*, 2012, **4**, 3174.
30 Y. Fan, X. Yang, Z. Cao, S. Chen and B. Zhu, *J. Appl. Electrochem.*, 2015, **45**, 131.
31 S. Manna, K. Das and S. K. De, *ACS Appl. Mater. Interfaces*, 2010, **2**, 1536.
32 S. Ghosh, M. Roy and M. K. Naskar, *Mater. Lett.*, 2014, **132**, 98.
33 S. K. Maji, N. Mukherjee, A. Mondal, B. Adhikary and B. Karmakar, *J. Solid State Chem.*, 2010, **183**, 1900.
34 L. Cheng, M. Shao, D. Chen and Y. Zhang, *Mater. Res. Bull.*, 2010, **45**, 235.
35 X. Chen, N. Q. Zhang and K. N. Sun, *J. Phys. Chem. C*, 2012, **116**, 21224.
36 J. Zhou, J. Dai, G. Q. Bian and C. Y. Li, *Coord. Chem. Rev.*, 2009, **253**, 1221.
37 M. Green and P. O'Brien, *Chem. Commun.*, 2000, 183.
38 N. K. Chaki, S. G. Sudrik, H. R. Sonawane and K. Vijayamohanan, *Chem. Commun.*, 2002, 76.
39 S. Mourdikoudis and L. M. Liz-Marzán, *Chem. Mater.*, 2013, **25**, 1465.
40 M. Jin, G. He, H. Zhang, J. Zeng, Z. Xie and Y. Xia, *Angew. Chem. Int. Ed.*, 2011, **50**, 10560.
41 M. Mohl, P. Pusztai, A. Kukovecz, Z. Konya, J. Kukkola, K. Kordas, R. Vajtai and P. M. Ajayan, *Langmuir*, 2010, **26**, 16496.
42 D. S. Wang, T. Xie, Q. Peng, S. Y. Zhang, J. Chen and Y. D. Li, *Chem. Eur. J.*, 2008, **14**, 2507.
43 G. Lin, W. Lu and W. Dong, *CrystEngComm*, 2013, **15**, 6690.
44 W. T. Yao, S. H. Yu and Q. S. Wu, *Adv. Funct. Mater.*, 2007, **17**, 623.
45 Q. Gao, P. Chen, Y. Zhang and Y. Tang, *Adv. Mater.*, 2008, **20**, 1837.
46 S. Sun, X. Zhang, J. Zhang, L. Wang, X. Song and Z. Yang, *CrystEngComm*, 2013, **15**, 867.
47 D. P. Singh, A. K. Ojha and O. N. Srivastava, *J. Phys. Chem. C*, 2009, **113**, 3409.
48 X. Xu, H. Yang and Y. Liu, *CrystEngcomm*, 2012, **14**, 5289.
49 K. K. Dey, A. Kumar, R. Shanker, A. Dhawan, M. Wan, R. R. Yadav and A. K. Srivastava, *RSC Adv.*, 2012, **2**, 1387.
50 Y. Zhao, J. Zhao, Y. Li, D. Ma, S. Hou, L. Li, X. Hao and Z. Wang, *Nanotechnology*, 2011, **22**, 115604.
51 S. O. Lee, R. Raja, K. D. Harris, J. M. Thomas, B. F. Johnson and G. Sankar, *Angew. Chem. Int. Ed.*, 2003, **42**, 1520.
52 S. E. Dapurkar, H. Kawanami, K. Komura, T. Yokoyama and Y. Ikushima, *Appl. Catal. A-Gen.*, 2008, **346**, 112.
53 Z. Y. Cai, M. Q. Zhu, J. Chen, Y. Y. Shen, J. Zhao, Y. Tang and X. Z. Chen, *Catal. Commun.*, 2010, **12**, 197.
54 H. Huang, H. Zhang, Z. Ma, Y. Liu, H. Ming, H. Li and Z. Kang, *Nanoscale*, 2012, **4**, 4964.

55 Y. Chang, Y. Lv, F. Lu, F. Zha and Z. Lei, *J. Mol. Catal. A-Chem.*, 2010, **320**, 56.
56 X. Cai, H. Wang, Q. Zhang, J. Tong and Z. Lei, *J. Mol. Catal. A-Chem.*, 2014, **383**, 217.
57 Y. Fu, D. Sun, M. Qin, R. Huang and Z. Li, *RSC Adv.*, 2012, **2**, 3309.
58 O. A. Kholdeeva, I. Y. Skobelev, I. D. Ivanchikova, K. A. Kovalenko, V. P. Fedin and A. B. Sorokin, *Catal. Today*, 2014, **238**, 54.
59 G. Tuci, G. Giambastiani, S. Kwon, P. C. Stair, R. Q. Snurr and A. Rossin, *ACS Catal.*, 2014, **4**, 1032.
60 J. Schaferhans, S. Gomez-Quero, D. V. Andreeva and G. Rothenberg, *Chem. Eur. J.*, 2011, **17**, 12254.
61 J. Dulle, K. Thirunavukkarasu, M. C. Mittelmeijer-Hazeleger, D. V. Andreeva, N. R. Shiju and G. Rothenberg, *Green Chem.*, 2013, **15**, 1238.
62 A. Carné, C. Carbonell, I. Imaz and D. Maspoch, *Chem. Soc. Rev.*, 2011, **40**, 291.
63 W. Xuan, C. Zhu, Y. Liu and Y. Cui, *Chem. Soc. Rev.*, 2012, **41**, 1911.